Article

Gas-Phase C–H and N–H Bond Activation by a High Valent Nitrido-Iron Dication and ⟨NH⟩-Transfer to Activated Olefins

Maria Schlangen, Johannes Neugebauer, Markus Reiher, Detlef Schrder, Jess Pitarch Lpez, Marco Haryono, Frank W. Heinemann, Andreas Grohmann, and Helmut Schwarz

J. Am. Chem. Soc., **2008**, 130 (13), 4285-4294 • DOI: 10.1021/ja075617w

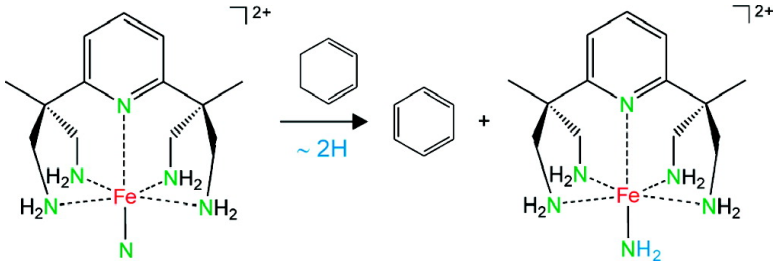

More About This Article

Additional resources and features associated with this article are available within the HTML version:

- Supporting Information
- Links to the 2 articles that cite this article, as of the time of this article download
- Access to high resolution figures
- Links to articles and content related to this article
- Copyright permission to reproduce figures and/or text from this article

View the Full Text HTML

J|A|C|S
ARTICLES
Published on Web 03/08/2008

Gas-Phase C−H and N−H Bond Activation by a High Valent Nitrido-Iron Dication and ⟨NH⟩-Transfer to Activated Olefins

Maria Schlangen,[#] Johannes Neugebauer,[‡] Markus Reiher,[‡] Detlef Schröder,[§,*] Jesús Pitarch López,[#] Marco Haryono,[#] Frank W. Heinemann,[⊥] Andreas Grohmann,[#,*] and Helmut Schwarz[#,*]

Institut für Chemie, Technische Universität Berlin, Strasse des 17. Juni 135, 10623 Berlin, Germany, Laboratory of Physical Chemistry, ETH Zürich, Wolfgang-Pauli-Strasse 10, 8093 Zürich, Switzerland, Institute of Organic Chemistry and Biochemistry, Flemingovo nám. 2, 16610 Prague 6, Czech Republic, and Institut für Anorganische Chemie, Universität Erlangen-Nürnberg, Egerlandstrasse 1, 91058 Erlangen, Germany

Received July 27, 2007; E-mail: detlef.schroeder@uochb.cas.cz

Abstract: A tetrapodal pentadentate nitrogen ligand (2,6-bis(1,1-di(aminomethyl)ethyl)pyridine, **1**) is used for the synthesis of the azido-iron(III) complex $[(\mathbf{1})Fe(N_3)]X_2$ where X is either Br or PF_6. By means of electrospray ionization mass spectrometry, the dication $[(\mathbf{1})Fe(N_3)]^{2+}$ can be transferred into the gas phase as an intact entity. Upon collisional activation, $[(\mathbf{1})Fe(N_3)]^{2+}$ undergoes an expulsion of molecular nitrogen to afford the dicationic nitrido-iron species $[(\mathbf{1})FeN]^{2+}$ as an intermediate, which upon further activation can intramolecularly activate C−H− and N−H bonds of the chelating ligand **1** or can transfer an ⟨NH⟩ unit in bimolecular reactions with activated olefins. The precursor dication $[(\mathbf{1})Fe(N_3)]^{2+}$, the resulting nitrido species $[(\mathbf{1})FeN]^{2+}$, and its possible isomers are investigated by mass spectrometric experiments, isotopic labeling, and complementary computational studies using density functional theory.

Introduction

The selective generation of high-valent transition-metal compounds forms a key motif in organometallic chemistry in general and oxidation catalysis in particular, because high-valent transition-metal species with a well-defined ligand environment may permit highly selective oxidation reactions or functionalizations of nonactivated hydrocarbons. In addition to oxidative dehydrogenation (e.g., ethylbenzene → styrene) as well as oxygenations (e.g., methane → methanol), an attractive target constitutes the direct N-functionalization of hydrocarbons via transfer of amido-, imido-, or nitrido-units (Scheme 1).

Established preparative methods for transition-metal-catalyzed direct C−N bond formation use precious metals, in particular palladium.[1] Iron, which plays a unique role in the Haber-Bosch process, is cheap and ecologically benign. It is therefore a prime candidate for catalyst development in sustainable chemical technology, and harnessing its activity for C−N bond coupling reactions would constitute a major step forward. One approach to uncover new types of reactions are investigations of highly reactive, bare metal ions in the idealized gas phase. Freiser and co-workers, who pioneered the chemistry of $FeNH_2^+$ and $FeNH^+$ cations, reported the first examples of C−N bond formation mediated by iron species,[2,3] but the bimolecular reactivity of bare iron-nitrido species has so far not been amenable to experimental study.[4] We therefore set out to provide an "ideal" coordination environment for the stabilization of a high-valent nitrido-iron species, making use of a highly symmetrical pentadentate, electron-donating nitrogen ligand, which leaves a sixth coordination site for the nitrido ligand, to give a complex of overall quasi-octahedral geometry. In the following, let us first summarize some salient features of iron coordination chemistry with nitrogen donor ligands, underscoring the particular properties of the chelate ligand used in this study.

Scheme 1. Metal-Mediated C−N Bond Formation with (a) Amido, (b) Imido, and (c) Nitrido Ligands.

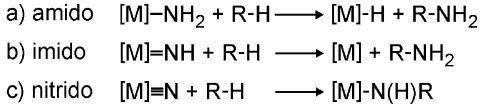

Whenever iron, ferrous or ferric, is present in a nitrogen-dominated coordination environment, the ligands usually contain imine donors or they are macrocyclic. Examples include species such as tris(phenanthroline)iron, hemeoglobin, and sarcophagine,[5] cyclam,[6] and triazacyclononane complexes.[7] These

[#] Technische Universität Berlin.
[‡] ETH Zürich.
[§] Institute of Organic Chemistry and Biochemistry.
[⊥] Universität Erlangen-Nürnberg.

(1) Buchwald, S. L.; Mauger, C.; Mignani, G.; Scholz, U. *Adv. Synth. Catal.* **2006**, *348*, 23.
(2) For $FeNH_2^+$, see: (a) Buckner, S. W.; Freiser, B. S. *J. Am. Chem. Soc.* **1987**, *109*, 4715. (b) Buckner, S. W.; Gord. J. R.; Freiser, B. S. *J. Am. Chem. Soc.* **1988**, *110*, 6606.
(3) For $FeNH^+$, see: (a) Schröder, D.; Hrušák, J.; Schwarz, H. *Ber. Bunsen. Phys. Chem.* **1993**, *97*, 1085. (b) Brönstrup, M.; Kretschmar, I.; Schröder, D.; Schwarz, H. *Helv. Chim. Acta* **1998**, *81*, 2348. (c) Brönstrup, M.; Schröder, D.; Schwarz, H. *Chem. Eur. J.* **1999**, *5*, 1176. (d) Liyanage, R.; Griffin, J. B.; Armentrout, P. B. *J. Chem. Phys.* **2003**, *119*, 8979. (e) Liyanage, R.; Armentrout, P. B. *Int. J. Mass Spectrom.* **2005**, *241*, 243.
(4) See also: (a) Fiedler, A.; Iwata, S. *Chem. Phys. Lett.* **1997**, *271*, 143. (b) Tan, L.; Liu, F. Y.; Armentrout, P. B. *J. Chem. Phys.* **2006**, *124*, 084302.

ligands either have π^* orbitals available for back-donation of electron density from the metal or at least ensure complex stability through the operation of the cryptate or macrocyclic effects. By way of extrapolation of this argument, we expect iron complexes with a large number of monodentate saturated nitrogen donor-ligands to be rare, as is indeed the case: the only example for which there is reliable evidence is the hexaammine complex $[Fe(NH_3)_6]^{2+}$.[8] Pentaammine complexes of iron have been studied theoretically[9] but never reproducibly prepared.[10] Such complexes are numerous for the heavier homologues of iron, that is, ruthenium and osmium, often containing extremely interesting ligands in the sixth coordination position. $[(NH_3)_5Ru(N_2)]^{2+}$ is the prototypical dinitrogen complex;[11] $[(NH_3)_5Ru(pyrazine)Ru(NH_3)_5]^{5+}$, the Creutz−Taube ion, has been studied extensively for its mixed valence and electron exchange characteristics,[12] and the high-yield preparation of organometallic $[(NH_3)_5Os(\eta^2\text{-}C_2H_4)]^{2+}$ attests to the fact that the pentaammine osmium(II) fragment binds π-bonding ligands such as olefins, acetylenes, and arenes with exceptional ease.[13]

Ammonia is a pure σ-donor ligand, hence the $[(NH_3)_5Fe]^{n+}$ fragment is expected to be electron-rich compared to other $[(L)_5Fe]^{n+}$ species, and may thus initiate unusual chemistry at the remaining coordination site. This reasoning prompted us to create the tetrapodal polyamine **1** which, as a chelating approximation of the pentaammine donor set, may to a large extent mimic the electronic properties of the $[(NH_3)_5Fe]^{n+}$ fragment.

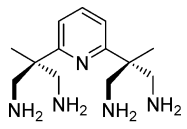

1

Ligand **1** readily forms complexes with both iron(II) and iron(III), allowing the stabilization of previously unknown bridging motifs, such as Fe^{II}-(OH)-Fe^{II}.[14] The ferrous κ-*N*-nitro complex shows unusual nitrite reductase-like reactivity,[15] and the related aqua complex can be oxidized cleanly with aerobic oxygen to give the diferric μ-oxo complex, without oxidative degradation of the ligand (such as unwanted imine formation).[16] When combined with a suitable monodentate N donor ligand in the sixth coordination position, iron(II) complexes of **1** undergo reversible spin transitions (between the low- and high-spin states, $S = 0$ and 2, respectively) in response to a change in temperature.[14,17]

The NN_4 ligand **1** thus provides the desired electron-rich square-pyramidal scaffold for the generation of octahedral iron complexes with all reactivity focused on the remaining sixth coordination site. In view of the recent advances in high-valent iron coordination chemistry, which were made using cyclam-derived macrocyclic ligands,[18−21] we were interested to probe the redox-innocence of **1**, and the accessibility of the pentavalent state. The present contribution reports the synthesis and characterization of the ferric azido complex $[(\mathbf{1})Fe(N_3)]Br_2$ and a detailed mass spectrometric and theoretical investigation of its fragmentation. The aim of this study is to probe whether the free, high-valent iron nitride $[(\mathbf{1})FeN]^{2+}$ is formed upon oxidative loss of dinitrogen from the azido ligand in the dication $[(\mathbf{1})Fe(N_3)]^{2+}$ according to reaction 1.

$$[(\mathbf{1})Fe(N_3)]^{2+} \rightarrow [(\mathbf{1})FeN]^{2+} + N_2 \qquad (1)$$

In a previous mass spectrometric study of the (cyclam-acetato)iron(III)-azido cation,[22] the evidence obtained indeed supported the formation of a nitrido-iron species as a short-lived intermediate, whereas the long-lived ions sampled after mass selection, probed in unimolecular as well as ion−molecule reactions, may be liable to further intracomplex rearrangements resulting in various C−H and N−H bond activation processes.

Experimental Section and Computational Details

All operations for the synthesis of the precursor compound $[(\mathbf{1})Fe(N_3)]Br_2$ were carried out under an atmosphere of dry dinitrogen, using dry solvents (<50 ppm H_2O), and chemicals from Aldrich and Acros used as received. $Na^{15}N_3$ (98%) was purchased from Chemotrade GmbH in Leipzig (Germany). To a suspension of **1**·4HBr·MeOH (280 mg, 0.461 mmol) in methanol (10 mL) was added LiOMe (1.8 mL of a 1 M stock solution in methanol, 1.8 mmol). The resulting clear solution was stirred for 5 min at room temperature. To this solution was added NaN_3 (30.0 mg, 0.461 mmol) dissolved in methanol (2 mL) followed by a solution of anhydrous $FeCl_3$ (74.8 mg, 0.461 mmol) in methanol (2 mL). The color of the solution turned red, and a precipitate of the same color formed. After stirring for 1 h at room temperature, the solid was collected by filtration, washed with diethyl ether, and dried in vacuo for 24 h (133.7 mg, 57%). The labeled compound was prepared in an analogous manner. Single crystals (used for the X-ray structure determination) of composition $[(\mathbf{1})Fe(N_3)](Br)(PF_6)\cdot H_2O$ were obtained from an aqueous solution of the dibromide salt containing an excess of NH_4PF_6. Anal. Calcd for ^{14}N-azide complex $C_{13}H_{25}Br_2Fe(^{14}N)_8\cdot 2CH_3OH$ (%): C, 31.43; H, 5.80; N, 19.55. Found: C, 32.05; H, 5.34; N, 19.83. Anal. Calcd for ^{15}N-azide complex $C_{13}H_{25}Br_2Fe(^{14}N)_5(^{15}N)_3\cdot 2CH_3OH$ (%): C, 31.28; H, 5.77; N, 19.96. Found: C, 31.90; H, 5.41; N, 19.83. IR (KBr) of $[(\mathbf{1})Fe(N_3)]Br_2$: $\tilde{\nu}$ [cm^{-1}] = 3181 (s), 3037 (s), 2929 (m), 2040 (s), 1964 (vs), 1595 (s), 1576 (s), 1470 (s), 1350 (m), 1205 (m), 1171 (s), 1100 (m), 1037 (s), 821 (s), 726 (m), 693 (m). Mössbauer data of $[(\mathbf{1})Fe(N_3)]Br_2$: $\delta_{Fe} = 0.27$ mm s^{-1}, $\Delta E_Q = 2.20$ mm s^{-1}, $\Gamma_- = 0.33(1)$, $\Gamma_+ = 0.33(1)$. The deuterium-labeled precursor ion $[(\mathbf{1_D})Fe(N_3)]^{2+}$ was prepared by dissolving $[(\mathbf{1})Fe(N_3)]Br_2$ in an excess of CH_3OD and storing the solution for 14 h at room temperature. In the resulting electrospray ionization (ESI) mass spectrum (see below), the signal due to $[(\mathbf{1})Fe(N_3)]^{2+}$ is cleanly shifted by plus eight mass

(5) Martin, L. L.; Martin, R. L.; Sargeson, A. M. *Polyhedron* **1994**, *13*, 1969.
(6) Berry, J. F.; Bill, E.; Bothe, E.; Neese, F.; Wieghardt, K. *J. Am. Chem. Soc.* **2006**, *128*, 13515.
(7) Song, Y.-F.; Berry, J.; Bill, E.; Bothe, E.; Weyhermueller, T.; Wieghardt, K. *Inorg. Chem.* **2007**, *46*, 2208.
(8) Behrens, H.; Wakamatsu, H. *Z. Anorg. Allg. Chem.* **1963**, *320*, 30.
(9) (a) Marynick, D. S.; Kirkpatrick, C. M. *J. Phys. Chem.* **1983**, *87*, 3273. (b) Kai, E.; Misawa, T.; Nishimoto, K. *Bull. Chem. Soc. Jpn.* **1980**, *53*, 2481.
(10) Mosbæk, H.; Poulsen, K. G. *Chem. Commun.* **1969**, 479.
(11) Senoff, C. V. *J. Chem. Educ.* **1990**, *67*, 368.
(12) Bolvin, H. *Inorg. Chem.* **2007**, *46*, 417.
(13) Smith, P. L.; Chordia, M. D.; Harman, W. D. *Tetrahedron* **2001**, *57*, 8203.
(14) Pitarch López, J.; Kämpf, H.; Grunert, M.; Gütlich, P.; Heinemann, F. W.; Prakash, R.; Grohmann, A. *Chem. Commun.* **2006**, 1718.
(15) Pitarch López, J.; Heinemann, F. W.; Prakash, R.; Hess, B. A.; Horner, O.; Jeandey, C.; Oddou, J.-L.; Latour, J.-M.; Grohmann, A. *Chem. Eur. J.* **2002**, *8*, 5709.
(16) Pitarch López, J.; Heinemann, F. W.; Grohmann, A.; Horner, O.; Latour, J.-M.; Ramachandraiah, G. *Inorg. Chem. Commun.* **2004**, *7*, 773.
(17) For a recent review on magnetic spin transitions, see: Sato, O.; Tao, J.; Zhang, Y.-Z. *Angew. Chem., Int. Ed.* **2007**, *46*, 2152.
(18) Meyer, K.; Bill, E.; Mienert, B.; Weyhermüller, T.; Wieghardt, K. *J. Am. Chem. Soc* **1999**, *121*, 4859.
(19) (a) Aliaga-Alcalde, N.; DeBeer George, S.; Mienert, B.; Bill, E.; Wieghardt, K.; Neese, F. *Angew. Chem., Int. Ed.* **2005**, *44*, 2908. (b) Petrenko, T.; et al. *J. Am. Chem. Soc.* **2007**, *129*, 11053.
(20) Berry, J. F.; Bill, E.; Bothe, E.; DeBeer-George, S.; Mienert, B.; Neese, F.; Wieghardt, K. *Science* **2006**, *312*, 1937.
(21) Chirik, P. J. *Angew. Chem., Int. Ed.* **2006**, *45*, 6956.
(22) Schröder, D.; Schwarz, H.; Aliaga-Alcalde, N.; Neese, F. *Eur. J. Inorg. Chem.* **2007**, *6*, 816.

units which is attributed to the exchange of all amino-hydrogen atoms for deuterium, that is, $[([all\text{-}ND_2]\text{-}\mathbf{1})Fe(N_3)]^{2+}$, $m/z = 178.5$, which we denote as $[(\mathbf{1_D})Fe(N_3)]^{2+}$ for simplicity. The ^{15}N labeled compound $[(\mathbf{1})Fe(^{15}N_3)]Br_2$was prepared in the same manner using $Na^{15}N_3$.

The mass spectrometric experiments were performed using a VG BIO-Q mass spectrometer as described in detail elsewhere.[23] Briefly, this machine is a commercial instrument which consists of an electrospray-ionization source combined with a tandem mass spectrometer of QHQ configuration (Q stands for quadrupole and H for hexapole). In the present experiments, millimolar solutions of $[(\mathbf{1})Fe(N_3)]Br_2$ dissolved in methanol were introduced through a fused-silica capillary into the ESI source with a syringe pump (ca. 2 μL min^{-1}). Nitrogen was used as a nebulizing and drying gas at a source temperature of about 80 °C. Maximum yields of the desired dication $[(\mathbf{1})Fe(N_3)]^{2+}$ and its labeled analogues $[(\mathbf{1_D})Fe(N_3)]^{2+}$ and $[(\mathbf{1})Fe(^{15}N_3)]^{2+}$ as well as the fragment ions due to loss of molecular nitrogen were achieved by adjusting the cone voltage between 10 and 40 V. For collision-induced dissociation (CID) at low collision energies, the ions of interest were mass selected using Q1, interacted with xenon as a collision gas in the hexapole under nearly single-collision conditions, typically 2×10^{-4} mbar, at variable collision energies ($E_{lab} = 0-20$ eV), while scanning Q2 to monitor the ionic products. Ion-reactivity studies of $[(\mathbf{1})FeN]^{2+}$ (and its isotopologs) with various neutral reagents were performed in the hexapole at an interaction energy nominally set to $E_{lab} = 0$ eV. In several previous studies, we have demonstrated that thermal reactivity can be monitored under these conditions.[24]

As pointed out previously, the VG Bio-Q does not allow directly to extract quantitative threshold information from CID experiments owing to several limitations of the commercial instrument.[23] For weakly bound ions for example,[25] even at $E_{lab} = 0$ eV a non-negligible amount of ion decay is observed, which is in part attributed to the presence of collision gas not only in the hexapole, but also in the focusing regions between the mass analyzers. Note that these dissociations do not correspond to metastable ions because they do not occur in the absence of collision gas. To a first approximation, however, the energy dependence of the product distributions in the CID spectra can be approximated by a sigmoid function,[26] which allows an extraction of some semiquantitative information about the energetics of the ions examined.[27] The energy dependence of the CID fragments can hence be approximated by functions of the type $I_i(E_{CM}) = (BR_i/(1 + e^{(E_{1/2,i}-E_{CM})b_i})$ using a least-square criterion; for the parent ion M, the relation is $I_M(E_{CM}) = [1 - \Sigma(BR_i/(1 + e^{(E_{1/2,i}-E_{CM})b_i})]$. Here, BR_i stands for the branching ratio of a particular product ion ($\Sigma BR_i = 1$), $E_{1/2}$ is the energy at which the sigmoid function has reached half of its maximum, E_{CM} is the collision energy in the center-of-mass frame ($E_{CM} = z \times m_T/(m_T + m_I) \times E_{lab}$, where z is the ion's charge, m_T and m_I stand for the masses of the collision gas and the ion, respectively), and b (in eV^{-1}) describes the rise of the sigmoid curve and thus the phenomenological energy dependence. In consecutive dissociations, all higher-order product ions were added to the intensity of the primary fragment. Further, non-negligible ion decay at $E_{lab} = 0$ eV as well as some fraction of nonfragmenting parent ions at large collision energies were acknowledged by means of appropriate scaling and normalization procedures. Phenomenological threshold energies are then derived from linear extrapolations of the rise of the sigmoid curves at $E_{1/2}$ to the baseline. This empirical, yet physically reasonable approach is able to reproduce the measured ion yields quite well. It is obvious, however, that the term $E_{1/2}$ used in the exponent does not correspond to the intrinsic appearance energies of the fragmentation of interest. Nevertheless, we have demonstrated in earlier work that this approach provides a quantitative frame for the energy demands of the various fragmentations.[24d,28,29]

In the computational studies, the molecular structures of all species were optimized using Kohn−Sham density functional theory (DFT) with the BP86 density functional[30] employing the resolution of identity (RI) technique.[31] The RI approach is a standard density-fitting technique that allows the reduction of the computational effort required for the calculation of two-electron integrals.[32] The results are hardly affected by this step while the benefit is an acceleration of the calculations by about 1 order of magnitude. Further, the triple-ζ plus polarization all-electron basis sets (TZVP) of Ahlrichs and co-workers were used for all atoms including iron[33] as implemented in the TURBOMOLE 5.1 suite.[34] The BP86 functional proved to be reliable with respect to structural parameters,[35,36] whereas the energetics of iron complexes with small high-spin/low-spin splittings are more difficult to treat.[37] As shown in a systematic study,[38] the energies for these kind of complexes obtained with pure density functionals differ largely from the results calculated with hybrid functionals. Thus, in addition to the pure density functional BP86, single-point calculations for every structure were carried out for comparison with the B3LYP hybrid functional,[37,39] whose energetic data is considered generally more reliable,[36] especially when different spin states are compared.[37,38] All optimized structures have been subjected to a frequency analysis to confirm the type of stationary point reached on the potential-energy surface. For this purpose we employed the seminumerical program package SNF.[40] To target the different spin states, we started unrestricted Kohn−Sham calculations with proper choices of the number of excess α-spin electrons. The unavoidable spin contamination was then assessed by inspection of the $\langle S^2 \rangle$ expectation value evaluated as in Hartree−Fock theory. Typical values of $\langle S^2 \rangle$ range from 0.76 to 0.95 for the doublet states and from 3.77 to 3.79 for the quartet states; increased expectation values are found for the doublet states of **4** (1.78), **5** (1.74), **6** (1.75), and **7** (1.60) and for the quartet states of **3** (4.20), **8** (4.10), and **9** (4.02); all values are given in the Supporting Information.

As the B3LYP//BP86 approach is of limited reliability for transition-metal complexes with the size of $[(\mathbf{1})Fe(N_3)]^{2+}$, we accordingly attempted to perform CCSD(T) calculations on these systems. Given that basis sets of TZVP quality need to be maintained, even with efficient quantum chemical codes and fast computers, these computations would, however, only be feasible with further structural simpli-

(23) Schröder, D.; Weiske, T.; Schwarz, H. *Int. J. Mass Spectrom.* **2002**, *219*, 729.
(24) (a) Schröder, D.; Schwarz, H.; Schenk, S.; Anders, E. *Angew. Chem., Int. Ed.* **2003**, *42*, 5087. (b) Roithová, J.; Hrušák, J.; Schröder, D.; Schwarz, H. *Inorg. Chim. Acta* **2005**, *358*, 4287. (c) Feyel, S.; Schröder, D.; Schwarz, H. *J. Phys. Chem. A* **2006**, *110*, 2647. (d) Schröder, D.; Engeser, M.; Schwarz, H.; Rosenthal, E. C. E.; Döbler, J.; Sauer, J. *Inorg. Chem.* **2006**, *45*, 6235. (e) Schröder, D.; Roithová, J.; Schwarz, H. *Int. J. Mass Spectrom.* **2006**, *254*, 197.
(25) Schröder, D.; Semialjac, M.; Schwarz, H. *Int. J. Mass Spectrom.* **2004**, *233*, 103.
(26) Bouchoux, G.; Leblanc, D.; Salpin, J. Y. *Int. J. Mass Spectrom.* **1996**, *153*, 37.
(27) Schröder, D.; Engeser, M.; Brönstrup, M.; Daniel, C.; Spandl, J.; Hartl, H. *Int. J. Mass Spectrom.* **2003**, *228*, 743.
(28) (a) Trage, C.; Diefenbach, M.; Schröder, D.; Schwarz, H. *Chem. Eur. J.* **2006**, *12*, 2454. (b) Gruene, P.; Trage, C.; Schröder, D.; Schwarz, H. *Eur. J. Inorg. Chem.* **2006**, *2006*, 4546.
(29) Jagoda-Cwiklik, B.; Jungwirth, P.; Rulíšek, L.; Milko, P.; Roithová, J.; Lemaire, J.; Maitre, P.; Ortega, J. M.; Schröder, D. *ChemPhysChem* **2007**, *8*, 1629.
(30) (a) Becke, A. D. *Phys. Rev. A* **1988**, *38*, 3098. (b) Perdew, J. P. *Phys. Rev. B* **1986**, *33*, 8822.
(31) (a) Eichkorn, K.; Treutler, O.; Öhm, H.; Häser, M.; Ahlrichs, R. *Chem. Phys. Lett.* **1995**, *240*, 283. (b) Eichkorn, K.; Weigend, F.; Treutler, O.; Ahlrichs, R. *Theor. Chem. Acc.* **1997**, *97*, 119.
(32) (a) Baerends, E. J.; Ellis, D. E.; Ros, P. *Chem. Phys.* **1973**, *2*, 41. (b) Dunlap, B. I.; Connolly, J. W. D.; Sabin, J. R. *J. Chem. Phys.* **1979**, *71*, 3396.
(33) Schäfer, A.; Huber, C.; Ahlrichs, R. *J. Chem. Phys.* **1994**, *100*, 5829.
(34) Ahlrichs, R.; Bär, M.; Häser, M.; Horn, H.; Kölmel, C. *Chem. Phys. Lett.* **1989**, *162*, 165.
(35) (a) Reiher, M.; Hess, B. A. *Chem. Eur. J.* **2002**, *8*, 5332. (b) Schatz, M.; Raab, V.; Foxon, S. P.; Brehm, G.; Schneider, S.; Reiher, M.; Holthausen, M.; Sundermeyer, J.; Schindler, S. *Angew. Chem., Int. Ed.* **2004**, *43*, 4360.
(36) Koch, W.; Holthausen, M. C. *A Chemist's Guide to Density Functional Theory*; Wiley-VCH: Weinheim, Germany, 2000.
(37) Reiher, M.; Salomon, O.; Hess, B. A. *Theor. Chem. Acc.* **2001**, *107*, 48.
(38) Salomon, O.; Reiher, M.; Hess, B. A. *J. Chem. Phys.* **2002**, *117*, 4729.
(39) (a) Lee, C.; Yang, W.; Parr, R. G. *Phys. Rev. B* **1988**, *37*, 785. (b) Becke, A. D. *J. Chem. Phys.* **1993**, *98*, 5648.
(40) Neugebauer, J.; Reiher, M.; Kind, C.; Hess, B. A. *J. Comput. Chem.* **2002**, *23*, 895.

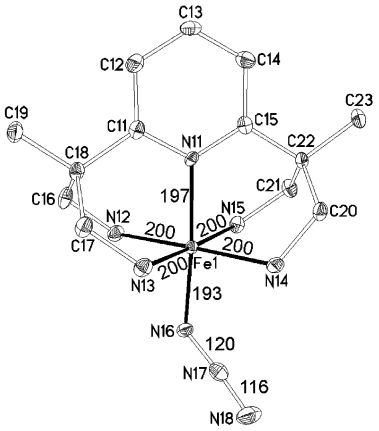

Figure 1. Molecular structure of the $[(\mathbf{1})Fe(N_3)]^{2+}$ dication in compound **2** (50% thermal ellipsoids); hydrogen atoms are omitted for clarity. Selected bond lengths are given in pm. Counterions are omitted.

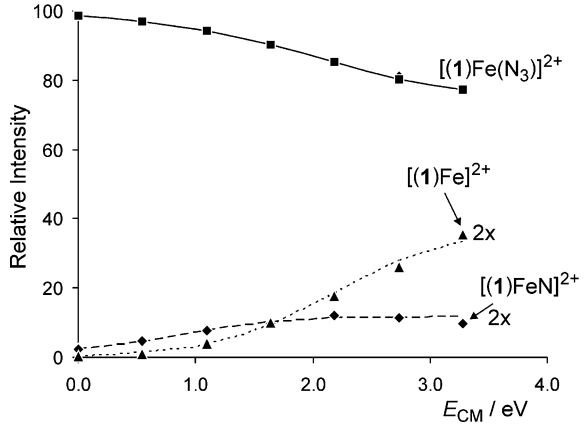

Figure 2. Relative intensities of the precursor dication $[(\mathbf{1})Fe(N_3)]^{2+}$ and the two most abundant fragments $[(\mathbf{1})FeN]^{2+}$ and $[(\mathbf{1})Fe]^{2+}$ upon CID of mass-selected $[(\mathbf{1})Fe(N_3)]^{2+}$ as a function of collision energy (E_{CM} given in eV in the center-of-mass frame). The symbols represent the experimental data for the parent ion $[(\mathbf{1})Fe(N_3)]^{2+}$ (■) and the primary fragments $[(\mathbf{1})FeN]^{2+}$ (♦) as well as $[(\mathbf{1})Fe]^{2+}$ (▲), whereas the lines show the fitting with sigmoid functions; see experimental details. Both fragment channels are expanded by a factor of 2.

fications. As an alternative, the energies of all structures were recalculated using the B3LYP* functional[37] which allows a more reliable calculation of spin-state splittings in transition-metal complexes. These additional results (see Supporting Information) show that the four most stable structures in the B3LYP calculation are also the most stable structures with B3LYP*, and their relative stabilities are conserved within less than ±20 kJ mol^{-1}. Moreover, the spin-state splittings do hardly change for these structures (between 8 and 12 kJ mol^{-1}), indicating that spin contaminations are not too severe. Also for the structures higher in energy, the spin-state splittings show changes of the order of 10 kJ mol^{-1} (with a maximum of 15 kJ mol^{-1}). Severe spin-contamination problems are only found for those structures that are energetically unfavorable anyway, so that they do not affect the conclusions of this work.

Results and Discussion

The precursor compound $[(\mathbf{1})Fe(N_3)]Br_2$ is prepared by addition of equimolar amounts of anhydrous $FeCl_3$ and NaN_3 to a methanolic solution of **1**·4HBr·MeOH and 4 equiv of LiOMe. The IR spectrum (KBr) of $[(\mathbf{1})Fe(N_3)]Br_2$ shows an intense band around 2040 cm^{-1}, which is assigned to the azide stretching vibration; similar values were found for related azido-iron(III) complexes.[18,41] The Mössbauer spectrum of $[(\mathbf{1})Fe(N_3)]Br_2$ at 77 K shows a doublet with an isomer shift $\delta_{Fe} = 0.27(1)$ mm s^{-1} and a quadrupole splitting of $\Delta E_Q = 2.20(1)$ mm s^{-1}, typical of an iron(III) low-spin complex and in agreement with the values found for a pair of related low-spin iron(III) azido complexes, namely *trans*-$[(cyclam)Fe^{III}(N_3)_2][ClO_4]$ ($\delta_{Fe} = 0.29(5)$ mm s^{-1}, $\Delta E_Q = 2.26(1)$ mm s^{-1}, 80 K) and $[(cyclam\text{-}acetato)Fe^{III}(N_3)][PF_6]$ ($\delta_{Fe} = 0.28(2)$ mm s^{-1}, $\Delta E_Q = 2.66(4)$ mm s^{-1}, 80 K).[18,41]

Single crystalline material has been obtained by recrystallization of $[(\mathbf{1})Fe(N_3)]Br_2$ from aqueous solution containing an excess of NH_4PF_6, affording the dicationic azido-iron complex $[(\mathbf{1})Fe(N_3)]^{2+}$ with one Br^- and one PF_6^- counterion as a monohydrate, $\{[(\mathbf{1})Fe(N_3)](Br)(PF_6)\cdot H_2O\}$, compound **2**, which crystallizes in the triclinic space group $P\bar{1}$ (No. 2). The dicationic core (Figure 1) has the iron center in the expected quasi-octahedral geometry, the charge being balanced by one bromide and one hexafluorophosphate anion. The distortions from ideal geometry are similar to those observed in the diferric μ-oxo complex.[16] The azido ligand is monodentate, coordinating the metal in trans-position with respect to the pyridine ring. The $Fe-N_{ligand}$ distances are all similar, ranging from 196.9(2) to 200.3(3) pm, which are typical values for $N-Fe^{III}$ bonds in iron complexes with low-spin ground states.[18,41] The Fe−N distance to the azido-nitrogen atom is 193.0(3) pm and thus shorter than the other Fe−N distances, as expected. The $Fe-N_3$ moiety is bent with the FeNN angle (126.6(2)°) deviating slightly from the value of 120° expected for an sp^2-hybridized nitrogen atom.

Under mild ionization conditions, ESI of a dilute methanolic solution of $[(\mathbf{1})Fe(N_3)]Br_2$ gives an intense signal for the dication $[(\mathbf{1})Fe(N_3)]^{2+}$ at $m/z = 174.5$ for the most abundant isotope (^{56}Fe) with the expected isotope pattern.[42] Collision-induced dissociation (CID) of mass-selected $[(\mathbf{1})Fe(N_3)]^{2+}$ gives two major ionic fragments with $m/z = 160.5$ and 153.5, respectively, over the range of collision energies studied, corresponding to losses of neutral molecules with the masses 28 and 42 amu, respectively (Figure 2).

In the CID spectra of the isotopologous $[(\mathbf{1_D})Fe(N_3)]^{2+}$, in which all four amino groups of the ligand are labeled with deuterium, and of the ^{15}N-labeled azido compound $[(\mathbf{1})Fe(^{15}N_3)]^{2+}$, the neutral fragments correspond to 28 and 42 amu for the former compared to 30 and 45 for the latter. These labeling patterns demonstrate that the azido group is eliminated in an oxidative (loss of N_2) and a reductive fashion (loss of N_3), reactions 1 and 2, respectively. The remaining five nitrogen atoms of the ligand **1** or conceivable combinations of other neutral molecules are obviously not involved in the gas-phase degradation of the dication $[(\mathbf{1})FeN_3]^{2+}$.

$$[(\mathbf{1})Fe(N_3)]^{2+} \rightarrow [(\mathbf{1})Fe]^{2+} + N_3 \qquad (2)$$

A more detailed consideration of the energy-dependent CID patterns in Figure 2 reveals the following. Loss of molecular nitrogen according to reaction 1 is already observed at a collision energy nominally set to $E_{CM} = 0$ eV, indicating that the activation energy of this process is rather low. In contrast, the loss of the azido ligand has a significantly higher energy

(41) Grapperhaus, C. A.; Mienert, B.; Bill, E.; Weyhermüller, T.; Wieghardt, K. *Inorg. Chem.* **2000**, *39*, 5306.

(42) Calculated with the Chemputer program developed by M. Winter, University of Sheffield; http://winter.group.shef.ac.uk/chemputer/.

demand, but then occurs more rapidly with increasing collision energy. Phenomenological analysis of the energy behavior leads to appearance energies of AE(1) = 0.1 ± 0.1 eV and AE(2) = 1.2 ± 0.2 eV for reactions 1 and 2; note that the AEs are affected by the lack of ion thermalization in our experiments as well as the kinetic energy spread of the incident beam and are thus only to be considered as a semiquantitative guidance.[29] The finding that N_2 loss dominates over the reductive elimination of N_3 at lower collision energies, whereas the opposite behavior prevails at higher energies, is in keeping with common understanding of unimolecular dissociations of gaseous ions:[43] The direct cleavage of the Fe−N_3 bond according to reaction 2 is entropically favored compared to an obviously more complex, but less energy demanding rearrangement accompanying the elimination of N_2 in reaction 1.

The key question which we will pursue in the following concerns the structure of the ionic fragment formed upon loss of molecular nitrogen from the dication $[(\mathbf{1})Fe(N_3)]^{2+}$. Specifically, we shall investigate whether the nitrido-iron(V) dication $[(\mathbf{1})FeN]^{2+}$ is formed as implied by reaction 1 or if the expulsion of N_2 is either immediately or in a subsequent process associated with rearrangement(s) to one or several isomeric ion(s) via insertion of the incipient nitrido-nitrogen atom into any of the accessible X−H or X−C bonds (X = C, N) of the ligand **1**. While mass spectrometry alone cannot provide an unambiguous answer in this respect, analysis of both the unimolecular fragmentation pattern and selected ion−molecule reactions, both aided by the investigation of labeled analogues, might give insight into the problem.[44] Further, computational studies with a focus on the energetics of isomers relevant in this context may prove helpful as demonstrated repeatedly in the past.[45] Therefore, we begin with the discussion of the relevant computational findings. Beforehand, we note that the computed structure of gaseous $[(\mathbf{1})Fe(N_3)]^{2+}$, the precursor used in the experiments, is in almost perfect agreement with the X-ray crystal structure. For the most stable doublet state, the Fe−N bond lengths of the four equatorial ligands are all very similar and amount to 203 pm (compared to 200 pm in Figure 1), the Fe−N distance to the pyridine nitrogen atom is computed as 200 pm (compared to 197 pm in Figure 1), and the Fe−N bond length to the azido ligand is computed as 190 pm (compared to 193 pm in Figure 1).

Dissociation of the precursor $[(\mathbf{1})Fe(N_3)]^{2+}$ according to reaction 1 to afford the nitrido species $[(\mathbf{1})FeN]^{2+}$ concomitant with N_2 formation is computed to be endothermic by 45 kJ mol^{-1}. In comparison, loss of the entire azido ligand to afford $[(\mathbf{1})Fe]^{2+}$ according to reaction 2 is predicted to be endothermic by 162 kJ mol^{-1} if the energetically lowest-lying triplet state of the dicationic fragment is formed. The computed endothermicities (0.47 and 1.68 eV, respectively) are somewhat larger than the experimental estimates of AE(1) = 0.1 ± 0.1 eV and AE(2) = 1.2 ± 0.2 eV, respectively, but the computed energetic order of both channels is consistent with the energy behavior of reactions 1 and 2 observed upon CID (Figure 2).[46] Further, the kinetic energy distribution of the incident ion beam as well as the distribution of internal energies are not treated explicitly in the determination of the AEs, such that the fitting procedure applied is likely to yield onsets lower than the corresponding thermochemical thresholds.[29] Despite these limitations of both theory and experiment, the differences of the fragmentation thresholds agree reasonably well, that is, $\Delta AE_{exp} = 1.1 \pm 0.2$ eV versus $\Delta AE_{th} = 1.21$ eV, which is fully consistent with the view that the effect of the ions' internal energy cancels in the direct competition of two fragmentation channels.[47] Further, the latter observation implies that the loss of N_2 from $[(\mathbf{1})Fe(N_3)]^{2+}$ occurs without a barrier in excess of the reaction endothermicity.

Let us now consider the nitrido species $[(\mathbf{1})FeN]^{2+}$ and some isomeric dications which all correspond to genuine minima; the energetic data given below refer to the B3LYP calculations and are given in kJ mol^{-1} relative to the precursor ion $[(\mathbf{1})Fe(N_3)]^{2+}$ with $E_{rel} = 0$ kJ mol^{-1}. Two spin states were considered, namely, $S = 0.5$ and $S = 1.5$. The high-spin/low-spin energy splittings are quite small (from 11 to 42 kJ mol^{-1}), and, as mentioned in the computational details, the energies for complexes with small spin splittings have to be taken with care.[48] Five types of structures were considered in the theoretical survey: (i) the high-valent iron-nitrido species $[(\mathbf{1})FeN]^{2+}$, denoted as structure **3** in Chart 1; (ii) isomeric species which result from insertion of the nitrido atom in various C−H and N−H bonds of the ligand **1**, eventually followed by further tautomerizations, while maintaining the formal iron(V) oxidation state, that is, structures **4**−**8**; (iii) species in which attack of the nitrido-nitrogen atom leads to the formation of a new N−N bond, structures **9** and **10**; (iv) dications in which new C−N bonds are formed by insertions of the nitrido-nitrogen atom, structures **11**, **12**, and **13**; and finally (v) structure **14**, in which a combined activation of adjacent C−H and N−H bonds leads to a imine substructure. In marked contrast to types i and ii, structures **9**−**14** all correspond to formal iron(III) compounds where the reduction of the valence state of the metal is associated with an oxidation of the ligand backbone. The most stable structure found, apparently the global minimum of the dication surface, corresponds to isomer **14**. In a chemical sense, the finding that **14** is the most stable of all structures considered in the theoretical work can be attributed to the quasi-octahedral coordination environment of the metal, its reduction from Fe(V) to Fe(III), and the formation of an imine unit which may serve as a favorable ligand for iron.

Notably, the formal iron(V) compounds resulting from primary H atom transfer from a neighboring C−H bond ($[(\mathbf{1})FeN]^{2+} \rightarrow \mathbf{8}$) or N−H bond ($[(\mathbf{1})FeN]^{2+} \rightarrow \mathbf{4}$) and possible subsequent hydrogen-atom transfers to the imido ligand (**4** → **5**, **4** → **6**, and **4** → **7**) are all similar in energy or even less stable than the nitrido species $[(\mathbf{1})FeN]^{2+}$. Specifically, the

(43) (a) Levsen, K. *Fundamental Aspects of Organic Mass Spectrometry*; VCH: Weinheim, Germany, 1978. (b) Gross, J. H. *Mass Spectrometry: A Textbook*; Springer-Verlag: Berlin, 2004.

(44) (a) Schröder, D.; Fiedler, A.; Hrušák, J.; Schwarz, H. *J. Am. Chem. Soc.* **1992**, *114*, 1215. (b) Schwarz, J.; Wesendrup, R.; Schröder, D.; Schwarz, H. *Chem. Ber.* **1996**, *129*, 1463.

(45) For selected examples, see: (a) Alcami, M.; Mó, O.; Yañez, M. *Mass Spectrom. Rev.* **2001**, *20*, 195. (b) Schwarz, H. *Int. J. Mass Spectrom.* **2004**, *237*, 75. (c) Mercero, J. M.; Matxain, J. M.; Lopez, X.; York, D. M.; Largo, A.; Erikson, L. A.; Ugalde, J. M. *Int. J. Mass Spectrom.* **2005**, *240*, 37. (d) The entire Vol. 201 of *Int. J. Mass Spectrom.* is dedicated to computational studies of ionic systems, see: Koch, W.; Hase, W. L. *Int. J. Mass Spectrom.* **2000**, *201*, 1.

(46) We note in passing that as a test for the accuracy of the functional, we also computed the bond dissociation energy $D(H-N_3)$ of free HN_3. The computed value of 356 kJ mol^{-1} reveals some underestimation compared to experiment (393 kJ mol^{-1}) which may be regarded as a minimal estimate for the uncertainty of the computational predictions for the system under study.

(47) Schröder, D.; Holthausen, M. C.; Schwarz, H. *J. Phys. Chem. B* **2004**, *108*, 14407.

(48) Note that for all structures, except for **8**, **10**, **13**, and **14**, the BP86 and B3LYP functionals predict the same multiplicity of the ground state.

Chart 1. BP86 Structures (Selected Bond Lengths in pm) and Relative Energies (B3LYP//BP86, in kJ mol^{-1}) for Doublet and Quartet States (in Parenthesis) of the Dications **3**−**14**[a]

Formal iron(V) compounds

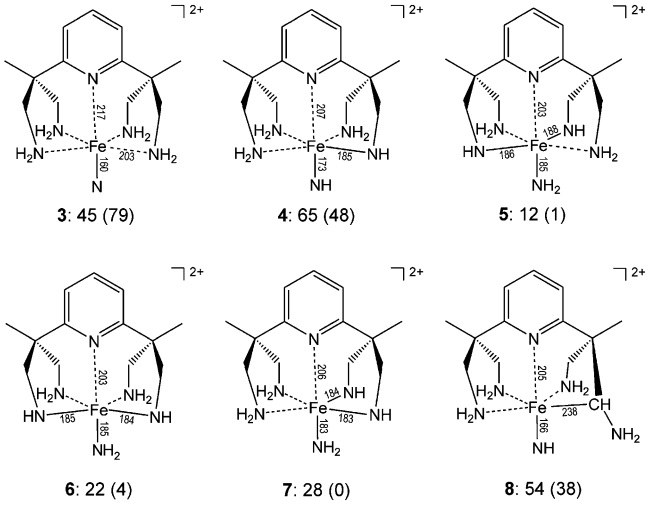

Formal iron(III) compounds

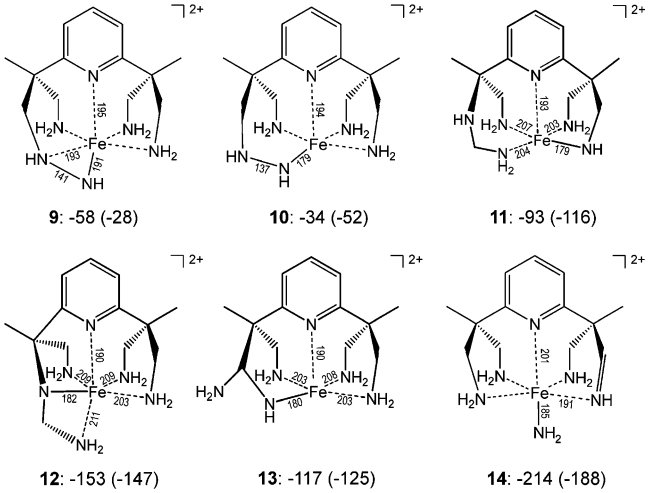

[a] All energies are given relative to the doublet ground state of $[(\mathbf{1})Fe(N_3)]^{2+}$ at 0 K and the liberated N_2 molecule must hence be included in the stoichiometric balance.

doublet state of the imido complex **4** is 20 kJ mol^{-1} less stable than doublet ^{2}**3**, and ^{4}**4** is almost isoenergetic to ^{2}**3**. The amido complexes **5**−**7** all have quartet ground states and are about 40 kJ mol^{-1} more stable than ^{2}**3**. While the doublet states of **5**−**7** show the expected energy order with compound ^{2}**5** bearing two trans-amido groups being most stable, the corresponding quartet states are very close in energy. As far as computed geometries are concerned, trends are as expected in that the covalent bonds to the nitrido ligand in ^{2}**3** (160 pm), the imido ligand in ^{2}**4** (173 pm), and the amido ligands in ^{2}**5**−^{2}**7** (between 183 and 188 pm) are all significantly shorter than the coordinative bonds between iron and the amino ligands (about 203 pm). An exception is the C−H insertion intermediate ^{2}**8** which has a rather long C−Fe distance (238 pm), most likely due to charge-transfer resulting in immonium character of the activated aminomethyl unit of the ligand. In marked contrast to the above structures, the isomers bearing N−N bonds (**9** and **10**) are considerably more stable than the putative precursor $[(\mathbf{1})FeN]^{2+}$

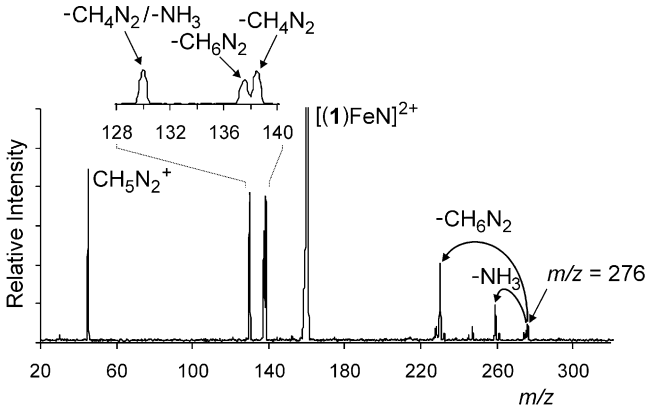

Figure 3. CID spectrum of the mass-selected dication with $m/z = 160.5$, formally corresponding to $[(\mathbf{1})FeN]^{2+}$, at a collision energy of $E_{CM} = 2.3$ eV. The intensity of the parent dication $[(\mathbf{1})FeN]^{2+}$ in the center of the spectrum is off-scale and ca. 30 times more intense.

and also lie well below the energy of the entrance channel, which can be attributed to the reduction of the metal to formal iron(III). Following this line of reasoning, it is not surprising that the isomers **11**−**14** with a new C−N bond are even more stable, because they also involve reduction to formal iron(III) and furthermore do not carry the disadvantage of an energetically unfavorable N−N single bond. The computed structures of isomers **9**−**14** follow the trends noted above, that is, significantly smaller bond distances between iron and the covalent ligands than for the coordinating amino group. Exceptions are **9** and **14**, where the former has a relatively long Fe−N bond (191 pm), which is attributed to strain resulting from the bidentate coordination to the hydrazido unit, and the short distance of only 191 pm between iron and the terminal imino ligand in **14**, which indicates some covalent character of the interaction. Obviously, a manifold of further isomers is conceivable (e.g., the *NH*-tautomers of **11**), and from the point of view of the entrance channel even the more energetic species are accessible from the precursor dication because most of them are lower in energy than $[(\mathbf{1})Fe(N_3)]^{2+}$. Due to the resulting structural complexity of the system, we have not undertaken more detailed theoretical studies aimed at locating all possible isomers, not to mention the investigation of the reaction pathways and the transition structures connecting the various isomers. Equipped with this information from theory, we will instead return to the experimental studies to sort out which of the above structures are chemically most reasonable to explain the experimentally observed patterns.

A typical collision-induced dissociation (CID) spectrum of the dication with $m/z = 160.5$ resulting from the loss of dinitrogen from the $[(\mathbf{1})Fe(N_3)]^{2+}$ precursor is shown in Figure 3; the assignments of the fragment compositions are based on the analysis of the CID spectra of the D_8− and ^{15}N labeled analogues (see below). At low collision energies, the dication undergoes loss of two different neutral fragments to afford dications with $m/z = 138.5$ and 137.5, which correspond to the eliminations of neutral $[CH_4N_2]$ and $[CH_6N_2]$, respectively. Another dicationic fragment ion at $m/z = 130$ in Figure 3 is due to a combined elimination of $[CH_4N_2]$ and NH_3 as derived from a parent-ion scan[49] of $m/z = 130$ and an independent CID experiment of the dication with $m/z = 138.5$, for which loss of neutral NH_3 is observed almost exclusively.

Scheme 2. C−C Bond Insertion of the Nitrido-Nitrogen Atom in **3** as a Key Step in the Fragmentation of $[(\mathbf{1})FeN]^{2+}$

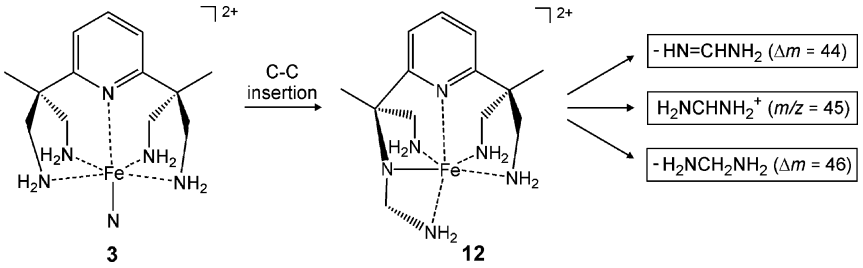

3 **12**

At elevated collision energies, charge separation of the $[(\mathbf{1})FeN]^{2+}$ dication takes place to afford two monocationic fragments. One of them has $m/z = 45$ and the elemental composition $CH_5N_2^+$, most probably the amino methanimmonium ion $H_2NCH{=}NH_2^+$,[50−52] rather than a hydrazine derivative. The formation of the $CH_5N_2^+$ fragment implies a direct relationship to the loss of neutral CH_4N_2 from the dication, because both channels are connected by simple proton transfer, and, irrespective of the actual structure of the CH_4N_2 unit, it can certainly be regarded as a strong base with a sizable proton affinity.[53] At low collision energies, the Coulomb barrier associated with the occurrence of proton transfer in the dication[54] cannot be surmounted and thus neutral CH_4N_2 is lost. Once sufficient energy is provided in CID, however, charge separation can take place and the $CH_5N_2^+$ fragment is formed efficiently. With regard to the second cationic counterpart, the situation shown in Figure 3 is more complex. Stoichiometry would require that charge separation of a $CH_5N_2^+$ cation from the $[(\mathbf{1})FeN]^{2+}$ dication leads to a $[C_{12}H_{20}N_4Fe]^+$ monocation with $m/z = 276$. This fragment is indeed observed in the high mass range of the CID spectrum (Figure 3), but several additional fragments are formed among which the most abundant are $[C_{12}H_{17}N_3Fe]^+$ ($m/z = 259$) and $[C_{11}H_{14}N_2Fe]^+$ ($m/z = 230$), corresponding to losses of ammonia and (formally) diaminomethane,[51] respectively, from the $[C_{12}H_{20}N_4Fe]^+$ monocation ($m/z = 276$).[55]

The assignments of the above compositions of the neutral and ionic fragments are based on the CID experiments with the labeled precursors for which the following mass shifts are observed.

(1) The dicationic fragments with $m/z = 137.5$ and 138.5 for $[(\mathbf{1})FeN]^{2+}$ do not experience any mass shift in the case of $[(\mathbf{1})Fe^{15}N]^{2+}$. Thus, the ^{15}N-label is included in the neutral CH_4N_2 and CH_6N_2 fragments lost. Beyond any doubt, this finding demonstrates that the nitrogen atom stemming from the azido ligand is distinguished from the other five nitrogen atoms of the ligand **1**, thereby excluding extensive H-migration steps which might eventually lead to an equilibration of all nitrogen atoms of the ligand. Starting from $[(\mathbf{1_D})FeN]^{2+}$, specific elimination of $CH_2D_2N_2$ is observed, whereas the elimination of neutral $CH_{6-n}D_nN_2$ is associated with H/D srcambling ($CH_4D_2N_2$, $CH_3D_3N_2$, and $CH_2D_4N_2$ are formed in a ratio of 53:100:38). The labeling patterns for $[(\mathbf{1})Fe^{15}N]^{2+}$ as well as $[(\mathbf{1_D})FeN]^{2+}$ thus indicate that the neutral CH_4N_2 fragment includes the nitrido-nitrogen atom and one of the four aminomethyl groups.

(2) The dicationic fragment with $m/z = 130$ and its origin in a two-step process (initial loss of neutral CH_4N_2 followed by expulsion of NH_3) is fully confirmed by the labeled precursor ions, that is, the fragment appears at $m/z = 132$ for $[(\mathbf{1_D})FeN]^{2+}$ and at $m/z = 130$ for $[(\mathbf{1})Fe^{15}N]^{2+}$.

(3) The signal at $m/z = 45$ is quantitatively shifted to $m/z = 48$ and $m/z = 46$ for $[(\mathbf{1_D})FeN]^{2+}$ and $[(\mathbf{1})Fe^{15}N]^{2+}$, respectively. This pattern is perfectly consistent with the already proposed relationship between the loss of neutral CH_4N_2 and the channel leading to $m/z = 45$ via proton transfer. The signals of the related monocations are also present in the spectra with the expected m/z values, that is, in the case of $[(\mathbf{1})Fe^{15}N]^{2+}$ no mass shifts are observed for the signals of $[C_{12}H_{20}N_4Fe]^+$ ($m/z = 276$), $[C_{12}H_{17}N_3Fe]^+$ ($m/z = 259$), and $[C_{11}H_{14}N_2Fe]^+$ ($m/z = 230$), whereas $[(\mathbf{1_D})FeN]^{2+}$ leads to $[C_{12}H_{15}D_5N_4Fe]^+$ ($m/z = 281$), $[C_{12}H_{14}D_3N_3Fe]^+$ ($m/z = 262$), and $[C_{11}H_{12}D_2N_3Fe]^+$ ($m/z = 232$).

The fragmentation behavior of $m/z = 160.5$ is thus in accordance with the initial generation of a genuine nitrido-iron dication $[(\mathbf{1})FeN]^{2+}$, and subsequent insertion of the nitrido nitrogen-atom into one of the tertiary C−C bonds of the ligands (**3** → **12**) can be considered as a key step to account for the experimentally observed fragmentations to afford neutral and cationic CH_nN_2 species as proposed in Scheme 2. Further, the occurrence of various C−H, C−C, and N −H bond activations as evidenced by the formation of products like CH_4N_2 and NH_3 is indicative of the presence of a highly reactive intermediate, which is capable of bond activation processes such as the "bare" imido-iron cation $FeNH^+$ or the related iron-oxide cation FeO^+.[3,56,57] It is of crucial importance to note, however, that while this chemical evidence very much supports the presence of the computationally predicted structure $[(\mathbf{1})FeN]^{2+}$ as an intermediate, it does not prove that the long-lived, nondecom-

(49) In a parent-ion scan, a first analyzer scans a regular mass spectrum, then the reaction of interest is allowed to occur in an intermediate collision cell, while a second mass analyzer is fixed to the mass of the desired product ion. In this way, all ions ("parents") giving rise to a particular product ion can be identified; for an example, see ref 24a.

(50) van Verth, J. E.; Saunders, W. H.; Kermis, T. W. *Can. J. Chem.* **1998**, *76*, 821.

(51) For the related diaminomethane, also see: DeBons, F. E.; Loudon, G. M. *J. Org. Chem.* **1980**, *45*, 1703.

(52) Exploratory DFT-calculations locate the isomers $CH_2NHNH_2^+$ and CH_3NHNH^+ as being 212 and 257 kJ mol^{-1}, respectively, less stable than $NH_2CHNH_2^+$.

(53) Hunter, E. P. L.; Lias, S. G. *J. Phys. Chem. Ref. Data* **1998**, *27*, 413.

(54) Roithová, J.; Herman, Z.; Schröder, D.; Schwarz, H. *Chem. Eur. J.* **2006**, *12*, 2465.

(55) The summed intensities of the monocationic metal-ion fragments ($m/z = 228-276$) adds up to slightly more than that of the $CH_5N_2^+$ fragment (ratio 1.2:1), which is a typical observation for charge-separation reactions of multiply charged ions to fragments of largely different masses and is due to differential collection efficiencies of the fragments formed upon Coulomb explosion in a beam-type mass spectrometer. See, for example: (a) Schröder, D.; Schroeter, K.; Schwarz, H. *Int. J. Mass Spectrom.* **2001**, *212*, 327. (b) Tsierkezos, N.; Schröder, D.; Schwarz, H. *J. Phys. Chem. A* **2003**, *107*, 9575. (c) Roithová, J.; Milko, P.; Ricketts, C. L.; Schröder, D.; Besson, T.; Dekoj, V.; Bělohradský, M. *J. Am. Chem. Soc.* **2007**, *129*, 10141.

(56) (a) Jackson, T. C.; Jacobsen, D. B.; Freiser, B. S. *J. Am. Chem. Soc.* **1984**, *106*, 1252. (b) Schröder, D.; Schwarz, H. *Angew. Chem., Int. Ed. Engl.* **1990**, *29*, 1433.

(57) Reviews on metal-oxide ions: (a) Schröder, D.; Schwarz, H. *Angew. Chem., Int. Ed. Engl.* **1995**, *34*, 1973. (b) Schröder, D.; Shaik, S.; Schwarz, H. *Struct. Bond.* **2000**, *57*, 91. (c) Schröder, D.; Schwarz, H. *Top. Organomet. Chem.* **2007**, *22*, 1.

Table 1. Relative Rate Constants (k_{rel})[a] and Products Formed in the Reactions of Various Neutral Molecules[b] with the Mass-Selected Dication with $m/z = 160.5$, Formally Corresponding to [(**1**)FeN]$^{2+}$, at a Collision Energy Nominally Set to $E_{lab} = 0$ eV

	k_{rel}[a]	products (branching)
CH_3OH	0.25	[(**1**)$FeCH_4NO]^+$ (100)
1,3-C_4H_6	0.02	[(**1**)$Fe]^{2+}$ + "C_4H_6N" (6)
		[(**1**−H)$Fe]^{2+}$ + "C_4H_7N" (1)
		[(**1**)$FeC_4H_6N]^{2+}$ (93)
c-C_6H_{10}	0.01	[(**1**−2H)$Fe]^+$ + $C_6H_{12}N^+$ (37)
		[(**1**)$FeC_6H_{10}N]^{2+}$ (63)
1,3-*c*-C_6H_8	0.28	[(**1**−2H)$Fe]^+$ + $C_6H_{10}N^+$ (20)
		[(**1**−H)$Fe]^{2+}$ + "C_6H_9N" (36)
		[(**1**)$FeC_6H_8N]^{2+}$ (44)
1,4-*c*-C_6H_8	1.00	[(**1**−2H)$Fe]^+$ + $C_6H_{10}N^+$ (40)
		[(**1**−H)$Fe]^{2+}$ + "C_6H_9N" (52)
		[(**1**)$FeC_6H_8N]^{2+}$ (8)

[a] Normalized to the fast reaction observed in the case of 1,4-cyclohexadiene. [b] In addition, ethene, propene, 1-butene, and *n*-butane were used as neutral reagents, and in all cases no significant reactivity was found ($k_{rel} < 0.01$).

posing ions sampled in the MS/MS experiments described here still exhibit this particular structure. In fact, the experimental data reported so far are consistent with several, but certainly not all of the computed isomeric structures (Chart 1).

To achieve further, independent insight, we attempted to probe the structure of [(**1**)FeN]$^{2+}$, $m/z = 160.5$, by investigating its ion−molecule reactions at thermal energy (Table 1). With *n*-butane as well as the simple alkenes ethene, propene, and 1-butene no reactions were observed at all, whereas a trace of a formal NH_2^+ transfer is observed in the case of cyclohexene along with prevailing association to the corresponding adduct. Likewise, adduct formation is observed with methanol, albeit with a significantly larger relative rate constant which can be assigned to the permanent dipole moment of this oxygen-containing ligand. It is to be noted that because of the design of our experimental setup, we cannot further characterize these formal adduct ions,[58] which either may correspond to electrostatically bound complexes of [(**1**)FeN]$^{2+}$ with the neutral reagents or may undergo complex rearrangements. With respect to the ion structure, the reactions with 1,3-butadiene and the two cyclic alkadienes, 1,3- and 1,4-cyclohexadiene are of particular interest. For the latter, in addition to adduct formation, two major processes occur, which correspond to formal transfers of $\langle NH_2^+ \rangle$ and $\langle NH \rangle$ units from the dication [(**1**)FeN]$^{2+}$ to the neutral dienes (reaction 3).

$$[(\mathbf{1})\mathrm{FeN}]^{2+} + C_6H_8 \rightarrow [(\mathbf{1}-2\mathrm{H})\mathrm{Fe}]^+ + C_6H_{10}N^+ \quad (3a)$$

$$\rightarrow [(\mathbf{1}-\mathrm{H})\mathrm{Fe}]^{2+} + \text{“}C_6H_9N\text{”} \quad (3b)$$

The charge-separation reaction (3a) corresponds to a formal $\langle NH_2^+ \rangle$ transfer to C_6H_8 and thus adds to the still few examples of bond-forming processes of multiply charged ions.[59] Starting from the deuterated precursor [(**1$_D$**)FeN]$^{2+}$, we observe clean transfer of $\langle ND_2^+ \rangle$, and [(**1**)$Fe^{15}N]^{2+}$ affords a specific transfer of $\langle {}^{15}NH_2^+ \rangle$ to the cyclohexadienes. Unfortunately, however, no conclusions can be drawn with regard to the structure of the $C_6H_{10}N^+$ monocations formed in reaction (3a). With respect to the structure of [(**1**)FeN]$^{2+}$, the clean transfer of $\langle ND_2^+ \rangle$ observed with [(**1$_D$**)FeN]$^{2+}$ excludes species in which the hydrogen atom of one of the C−H bonds has been transferred to the nitrido nitrogen-atom, while the ^{15}N label proves the specific position of this nitrogen atom compared to those contained in ligand **1**.

Scheme 3. Transfer Hydrogenation Proposed for the Reaction of [(**1**)FeN]$^{2+}$ with Cyclohexadienes (Only 1,3-Cyclohexadiene Is Shown Here)

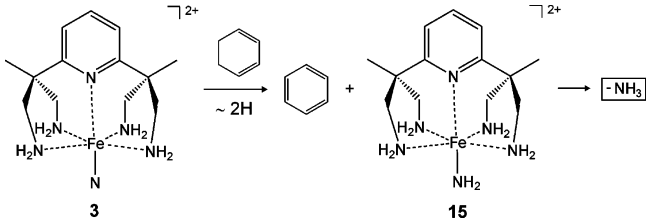

3 **15**

Similar to the fragmentation processes described above, the formal ⟨NH⟩ transfer occurring in reaction 3b, a bond-forming reaction of a molecular dication with conservation of the 2-fold charge,[59] is related to reaction 3a via simple proton transfer. Fully consistent with this relationship, the labeling patterns reveal specific transfers of ⟨ND⟩ and $\langle {}^{15}NH \rangle$ from [(**1$_D$**)FeN]$^{2+}$ and [(**1**)$Fe^{15}N]^{2+}$, respectively, to the cyclohexadienes. As far as the neutral "C_6H_9N" product formed in reaction 3b is concerned, formation of benzene and ammonia appears most likely from a thermochemical point of view.[60] However, with respect to the observed formation of an intact $C_6H_{10}N^+$ species in reaction 3a, the formation of a less stable "C_6H_9N" isomer also cannot be ruled out. A more definitive assignment by mass spectrometric means would require more sophisticated experiments,[61] which cannot be applied in this particular case for instrumental circumstances. Tentatively, for the potential generation of $C_6H_6 + NH_3$, we propose that in the ensuing ion−molecule complex the nitrido-nitrogen atom abstracts two hydrogen atoms from the "hydrogen pool" of cyclohexadiene, coupled with the liberation of benzene (**3** → **15**), followed by hydrogen migration from one of the NH_2 groups of the ligand **1** and eventual elimination of NH_3 (Scheme 3).

$$[(\mathbf{1})\mathrm{FeN}]^{2+} + C_4H_6 \rightarrow [(\mathbf{1})\mathrm{Fe}]^{2+} + C_4H_6N^{\bullet} \quad (4)$$

Most intriguing as far as ion structures are concerned is a minor pathway corresponding to N atom transfer in the case of 1,3-butadiene (reaction 4), Figure 4a. To prove that this reaction indeed corresponds to a genuine N atom transfer, the reactions of the ^{15}N-labeled dication [(**1**)$Fe^{15}N]^{2+}$ with 1,3-butadiene (Figure 4b) and of [(**1**)FeN]$^{2+}$ with the deuterated substrate [1,1,4,4-D_4]-1,3-butadiene (Figure 4c) were investigated as well. The results of these experiments are both consistent with the expected product patterns of a reaction according to reaction 4.

Let us now return to the structure of the [(**1**)FeN]$^{2+}$ dication, specifically the question whether this species has retained structure **3** of the elusive nitrido-iron complex, or whether post-collisional rearrangements have taken place, as has been proposed in the case of [(cyclamacetato)FeN]$^+$.[22] In brief, the structural evidence gained from the CID experiments and the

(58) Feyel, S.; Schröder, D.; Rozanska, X.; Sauer, J.; Schwarz, H. *Angew. Chem., Int. Ed.* **2006**, *45*, 4677.
(59) Roithová, J.; Schröder, D. *Phys. Chem. Chem. Phys.* **2007**, *9*, 2341.
(60) NIST Standard Reference Database Number 69, Gaithersburg, MD, 2005, http://webbook.nist.gov/chemistry/.
(61) Neutralization-reionization mass spectrometry has been used to characterize the organic products formed in metal-mediated reactions in the gas phase, see: (a) Schröder, D.; Sülzle, D.; Hrušák, J.; Böhme, D. K.; Schwarz, H. *Int. J. Mass Spectrom. Ion Processes* **1991**, *110*, 145. (b) Schröder, D.; Schwarz, H. *Helv. Chim. Acta* **1992**, *75*, 1281.

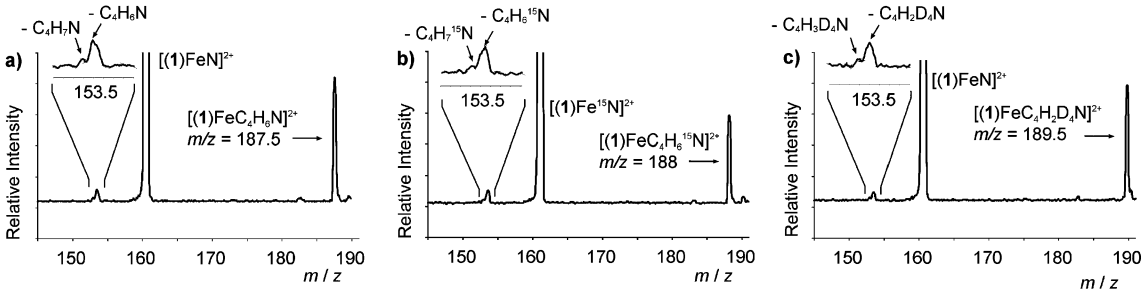

Figure 4. Spectra of the ion−molecule reactions of (a) $[(\mathbf{1})FeN]^{2+}$ with 1,3-butadiene; (b) $[(\mathbf{1})Fe^{15}N]^{2+}$ with 1,3-butadiene; (c) $[(\mathbf{1})FeN]^{2+}$ with [1,1,4,4-D_4]-1,3-butadiene. The intensities of the parent dications $[(\mathbf{1})FeN]^{2+}$ and $[(\mathbf{1})Fe^{15}N]^{2+}$, respectively, are off-scale and ca. 80 times more intense.

Scheme 4. Proposed Mechanism for the N Atom Transfer Observed in the Reaction of $[(\mathbf{1})FeN]^{2+}$ with 1,3-Butadiene

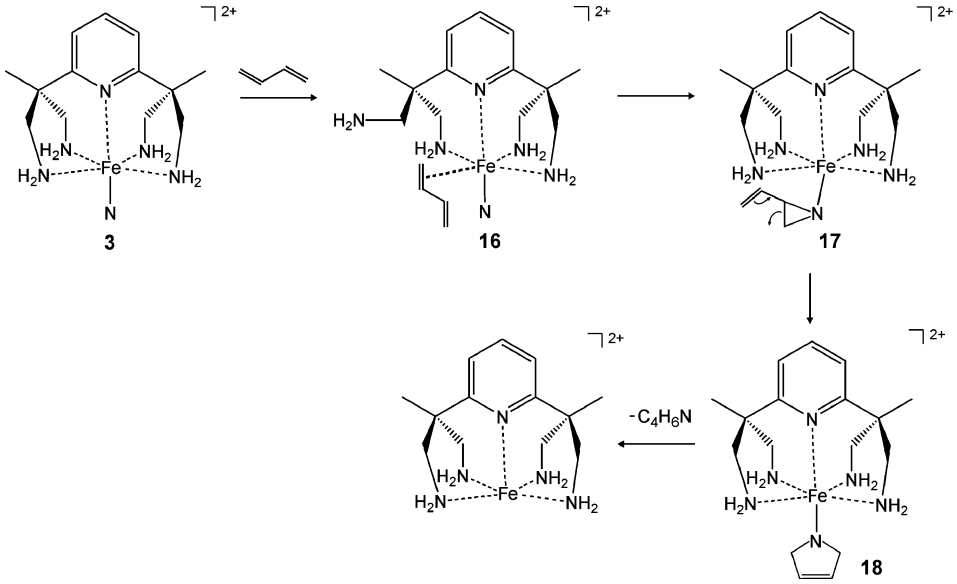

reactivity studies can be summarized as follows. (i) The nitrido nitrogen atom retains its identity, that is, there is no evidence for an equilibration with the nitrogen atoms of the amino groups. Moreover, this particular nitrogen atom is exclusively involved in the formal ⟨NH⟩ and $\langle NH_2^+\rangle$ transfer processes observed with acyclic and cyclic dienes. Hence, of structures **3**−**14** in Chart 1, at least **11**−**13** appear less likely candidates to account for the experimental findings. (ii) Exclusive transfers of ⟨ND⟩ and $\langle ND_2^+\rangle$ with the deuterated species $[(\mathbf{1_D})FeN]^{2+}$ rule out the occurrence of C−H activation, such that we can further exclude structure **8** and also that of the apparent global minimum **14**. (iii) For the remaining isomers, the observed ⟨NH⟩ and $\langle NH_2^+\rangle$ transfers are consistent with isomers **4**−**7**, whereas no evidence points toward N−N bond formation such as in **9** and **10**. Last but not least, (iv) even though the corresponding peaks in Figure 4 are only minor, the observed N atom transfer to butadiene according to reaction 4 does in fact provide direct evidence for the assumption that $[(\mathbf{1})FeN]^{2+}$ does indeed have the intact structure **3** and that the further rearrangements are only induced in the ion/molecule reactions or upon collisional excitation in CID. We accordingly suggest that at least part of the ions formed from $[(\mathbf{1})Fe(N_3)]^{2+}$ upon loss of dinitrogen corresponds to the free nitrido species **3**. If this hypothesis is correct, why then is the reactivity of **3** so limited as to react only with dienes and not with saturated hydrocarbons nor with simple alkenes? Quite obviously, thermodynamic reasons cannot be put forward, because the drastically increased stabilities of the iron(III) compounds in Chart 1 leave no doubt that the nitrido complex has a high potential to react with organic substrates. Instead, we propose that the particular structure of **3** with a quasi-octahedral environment of the metal constrains the reactivity to those substrates which are able to replace one of the aminomethyl groups of the chelating ligand in the coordination sphere, before any further reactions can occur. Thus, the binding energy of bare Fe^+, which is the closest analogy to ligated Fe^{2+} for which the corresponding data are available in the literature, to 1,3-butadiene is significantly larger (181 ± 7 kJ mol^{-1})[62] than that of Fe^+ to ethene (145 ± 6 kJ mol^{-1}),[63] and comparable to that of Fe^+ to ammonia (184 ± 12 kJ mol^{-1}),[64] such that butadiene may at least temporarily replace an aminomethyl substituent in the collision complex, for which we can also expect an entropic advantage due to the release of strain in the chelating ligand. Following this line of reasoning, we can also propose a possible mechanistic rationale for the bimolecular reactions reported in Table 1. In the reaction of dication **3** with butadiene (Scheme 4), the hydrocarbon first binds to the metal by replacing one of the coordinating aminomethyl arms. In the so-formed structure **16**, the C═C double bonds of the substrate are in the vicinity of the nitrido unit which eventually allows for the formation of an intermediate aziridinyl group assisted by a

(62) Schröder, D.; Schwarz, H. *J. Organomet. Chem.* **1995**, *504*, 123.
(63) Sievers, M. R.; Jarvis, L. M.; Armentrout, P. B. *J. Am. Chem. Soc.* **1998**, *120*, 1891.
(64) Walter, D.; Armentrout, P. B. *J. Am. Chem. Soc.* **1998**, *120*, 3176.

rebound of the fourth aminomethyl ligand (**16** → **17**). The unstable aziridine may then undergo an electrocyclic rearrangement with assistance by the metal center[65] to afford a dihydropyrrol unit in **18**, followed by release of a neutral C_4H_6N radical.

The most important conclusion derived from the reaction with butadiene is that these results strongly indicate the $[(\mathbf{1})FeN]^{2+}$ species having retained its initial structure **3** also in the long-lived ion sampled in the reactivity studies. Hence, we have strong evidence that our initial strategy, which led us to choose the electron-rich, spatially restricted nitrogen ligand **1** for the stabilization of a gaseous iron-nitrido species, has been indeed successful.

Conclusions

Owing to the stabilizing tetraaminoimine **1** and the mildness of electrospray mass spectrometry, the azido iron(III) species $[(\mathbf{1})Fe(N_3)]^{2+}$ can exist as a long-lived molecular dication in the gas phase. Collisional activation of $[(\mathbf{1})Fe(N_3)]^{2+}$ leads to the bare iron-nitrido dication $[(\mathbf{1})FeN]^{2+}$ as an intermediate with formally high-valent Fe(V). In contrast to an earlier related work on the [(cyclam-acetato)FeN]$^+$ monocation,[22] the fragmentation patterns as well as reactivity studies are consistent with the structure of an intact iron-nitrido species, rather than the occurrence of suicidal oxidation of the chelate ligand **1**. In fact, gaseous $[(\mathbf{1})FeN]^{2+}$ is capable of transferring an ⟨NH⟩ unit to activated alkenes; due to the dicationic nature of $[(\mathbf{1})FeN]^{2+}$, the reactions can be accompanied by charge-separation processes via simple proton transfer to afford a pair of monocationic products, resulting in formal transfer of $\langle NH_2^+ \rangle$. In the case of butadiene, the observation of an N atom transfer provides even more direct evidence for the persistence of the nitrido structure. The experimental results are further backed up by density functional calculations which fully support the proposed scenario. More detailed insight into the mechanisms of the mutual interconversions of the various isomers would be gained if all transition structures were localized, but given the size of the system under study and the number of relevant minima (Chart 1), such an effort is far beyond the scope of this study. Notwithstanding the chemical evidence for the structure of $[(\mathbf{1})FeN]^{2+}$ provided in this work, more specific means for the distinction of isomeric structures would be desirable. In this respect, infrared spectroscopy of the mass-selected $[(\mathbf{1})FeN]^{2+}$ dication might be particularly informative.[29,55c,66,67]

Acknowledgment. Dedicated to Horst Kirsch on the occasion of his 65th birthday. This work was supported by the Czech Academy of Sciences (Grant Z40550506), the Deutsche Forschungsgemeinschaft (SFB 658), the Grant Agency of the Academy of Sciences of the Czech Republic (Grant KJB400550704), and the Fonds der Chemischen Industrie.

Supporting Information Available: Full details of ref 19b, relative B3LYP and B3LYP* energies, spin expectation values, the Cartesian coordinates of the computed structures, and a cif-file of the X-ray data. This material is available free of charge via the Internet at http://pubs.acs.org.

JA075617W

(65) Schroeter, K.; Schalley, C. A.; Schröder, D.; Schwarz, H. *Organometallics* **1997**, *16*, 986.

(66) (a) Schröder, D.; Schwarz, H.; Milko, P.; Roithová, J. *J. Phys. Chem. A* **2006**, *110*, 8346. (b) Feyel, S.; Schwarz, H.; Schröder, D.; Daniel, C.; Hartl, H.; Döbler, J.; Sauer, J.; Santambrogio, G.; Wöste, L.; Asmis, K. *ChemPhysChem* **2007**, *8*, 1640.

(67) (a) Dopfer, O. *J. Phys. Org. Chem.* **2006**, *19*, 540. (b) Polfer, N. C.; Oomens, J. *Phys. Chem. Chem. Phys.* **2006**, *9*, 3804.